DARPA
Instant Flame Suppression
Phase II – Final Report

Harvard University

- Electrostatics -

Introduction

The flames of hydrocarbons produce charged species through two mechanisms: thermal ionization and chemiionization.[1] Of the two processes, the latter one is dominant. The resulting steady state concentration of charges in a hydrocarbon flame ranges between 10^9 cm^{-3} and 10^{11} cm^{-3}.

The chemical nature of the charges is very heterogeneous. The chemiionization reaction is thought to be $CH + O \rightarrow CHO^+ + e^-$. The two charged species quickly react (gas phase reactions involving ions have typically much higher rates than reactions among analogous but neutral species) generating a diverse population of ions.

An electric field will exert a force on these charges and will confer momentum to them.[2] This momentum is transferred to neutral species whenever these collide with an accelerated charged specie. The momentum imparted to the charged species in a flame by electric fields can, in principle, generate macroscopic flows within the flame. This phenomenological picture serves as a rationale for the study of the effects of electric fields on flames.[2] The force exerted by the electric field force will depend on the local intensity of the field. In the case of a polarizable cloud of charge (our flame), the local fields can be strongly affected by the spatial distribution of the other charges. This screening effect is considered responsible for the minute magnitude of the effects displayed by DC electric fields on flames.

In phase I we have shown that AC fields can lead to effects that are larger than those exhibited by DC fields. As we have shown in our Phase II efforts, this difference in behavior arises from differences in the screening response of the charges in the flame, and from differences in the effect of system geometry.

Phase Space Determination

Summary. In Phase I we showed that inhomogeneous AC fields can lead a flame to be deflected towards regions of high field density or low field density, depending on the frequency of the field. In the latter case, at high field intensities, we showed how the deflection could be sufficient to blow off a methane/air conical non-premixed flame from a 3mm burner. Nonetheless, the low throughput of the experimental protocols we were using was compromising our ability to have a complete picture of the phenomenon.

To facilitate the development of experimental information on the influence of the key parameters on the response of the flame, we devised a computerized system (Figure 1) that allowed for the automated measurement of the angle of deflection of a flame as a function of the voltage applied on the electrode (i.e. field applied on the flame) and the frequency of the field oscillations.

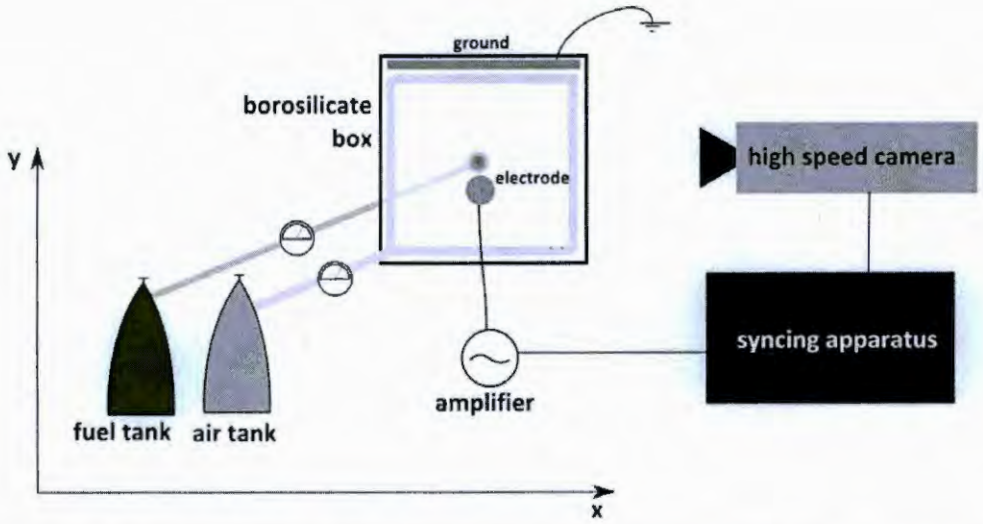

Figure 1. Sketch in top view of the apparatus devised to sample the voltage/frequency parameter space on the deflection of the flame from a point electrode.

Experimental Details. To simplify the definition of the magnitude of the field at the flame, we opted for bare metal electrodes in the form of 1 inch spheres. These electrodes would not generate ionic wind. Compared to wire electrodes previously used in our experiments, the spherical electrodes would not be reaching the same field intensities at short distances. Nonetheless, high field intensities are important for the study of flame suppression; suppression occurs with increasing likelihood at increasing field strengths. Lower fields are sufficient for the study of deflection.

As shown in Figure 1 the flame (methane/air conical non-premixed) is generated within a transparent square box (35 cm sides) by a ceramic burner embedded in its base. The mouth of the burner is circular in shape and 3 mm wide. The bottom internal perimeter of the box is lined with a flexible bubbler for aquariums, connected to an air tank; the uniform air flow generated by the bubbler is used to stabilize the flame. The methane flowing to the burner and the air flowing to the bubbler are regulated by separate mass flow controllers.

The spherical electrode was made of steel and connected to a steel rod. The steel rod was immobilized within a custom printed sample holder. The steel rod was electrically connected to the high voltage amplifier. The input to the amplifier was generated by a Labview board which was further connected to a high speed camera. The board was controlled through a laptop.

Through this setup, we were able to sample the parameter space (voltage vs frequency vs deflection) with arbitrary granularity. Each field condition would be characterized by 7 pictures (separated by 50 ms) collected by the high speed camera.

The protocol adopted for the calculation of the deflection angle from the images is shown in Figure 2.

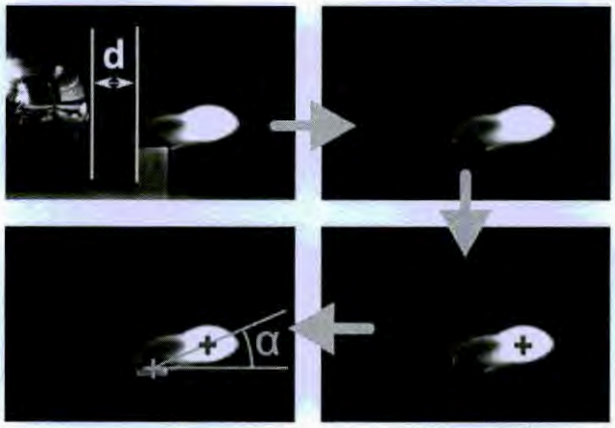

Figure 2. Image processing protocol for the determination of flame deflection from automated image collection system.

Beside deflection angle we could quantify the luminosity of the flame, as measured by the detector of the camera. While the luminosity associated with each pixel is a function of the sensitivity of the camera, we interpret the value of luminosity as an indication of the amount of soot present in the flame, since most of the visible light emitted by a methane flame originates from the black body radiation of the soot.

Results and Discussion. The resulting plots allowed us to get a coherent picture of the parameter space of the phenomenon. The different rows in Figure 3 shows the 3d plots obtained through our procedure: the deflection of the flame, the standard deviation associated with the deflection, and the luminosity. The abscissa is the voltage (from 0 kV to 30 kV), while the ordinates is the frequency (from 50 Hz to 3000Hz, on a log scale). The third axis is depicted in all plots through a color map (for deflection, blue = -90 degrees and red = 90 degrees; for the standard deviation to deflection, blue = 0% and red = 30%; for luminosity, blue = minimum and red = maximum). In these plots we chose to define the deflection angle from the vertical: positive angles indicate the angles by which the flame is deflected from the vertical in the direction opposite to the electrode, while negative angles indicate the angle by which the flame is deflected from the vertical towards the electrode. The uniformly colored triangle in the top right corner (corresponding to high voltages and high frequencies) consists of conditions that could not be explored due to the limited slew rate of the amplifier. The two columns in Figure 3 show two different experiments conducted in the same conditions to demonstrate the reproducibility of our experiments.

The deflection plots show that, in the conditions of this experiment, repulsion of the flame from the electrode occurs from 15 kV onwards, largely irrespectively of frequency. Nonetheless, as the voltage increases, the repulsion shows a positive frequency dependence (i.e., higher deflection at higher frequencies). The attraction of the flame is concentrated at an intermediate range of voltages and frequencies (the center of the plot).

The plots of the standard deviation of the flame show that the oscillations of the flame increase in magnitude as the field increases, leading to a higher error in the determination of the deflection from a

finite number of replicates. This is especially the case when the frequency of the field is very low (<100 Hz).

A general observation from the plot of luminosity shows that the application of strong electric fields decreases the luminosity of the flame. Furthermore, it shows a strong dependence of the visible luminosity of the flame as a function of frequency and voltage. Interestingly, at the highest field strengths, the luminosity increased with increasing deflection. If we assume that the luminosity determined by the camera is a measure of the amount of soot in the flame, this plot suggests that the increase in positive deflection of the flame at high frequencies and high voltages (and, therefore, its eventual suppression) is correlated with the persistence of soot in the flame. The decrease in luminosity at high voltages and low frequencies could be interpreted in two ways: i) the soot is ejected from the flame before it has time to heat up, or ii) the flame produces less soot.

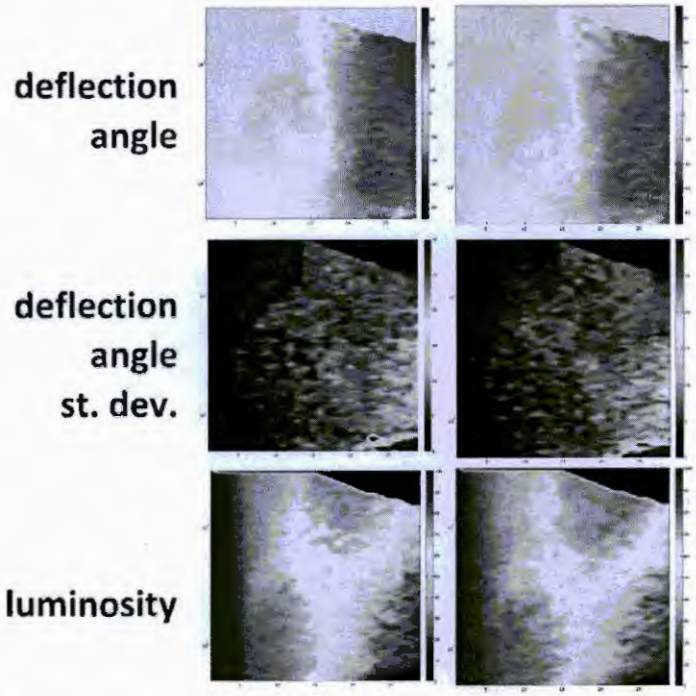

Figure 3. 3d plots of deflection, standard deviation of deflection, and luminosity as functions of voltage and frequency of the electric field. The two columns correspond to two different experiments conducted in the same set of conditions (electrode: 1" sphere; waveform: sine; fuel: CH_4; oxidizer: air; fuel flow: 30 ml/min; burner diameter: 1/8").

By knowing the distance of the electrode from the flame, it is possible to calculate the intensity of the electric field at the location of the flame. In Figure 4 is shown the deflection of the flame as a function of electric field intensity (at the flame) for several electrode-flame distances and constant frequency (1500Hz).

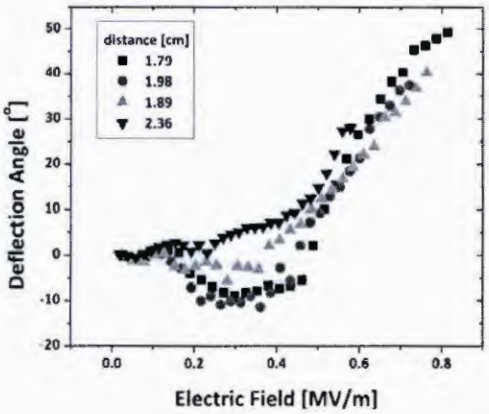

Figure 4. Deflection of the flame as a function of electric field intensity at the flame for different electrode-flame distances.

Despite the obviously low accuracy of the estimation of the intensity of the field at the flame in these conditions, the way in which the curves obtained from different experiments overlap is quite encouraging. The plot shows that at low electric fields (<0.1 MV/m) the deflection is small but positive. Between 0.1 MV/m and 0.5 MV/m the deflection turns negative. Interestingly, the extent of deflection for the same field at the flame depends on the relative distance between the electrode and the flame: attraction of the flame to the electrode is more effective when the electrode is close to the flame. Above 0.5 MV/m the plots converge, the deflection becomes positive and steadily increases with increasing field intensity.

These results suggest that, in the case of a bare electrode and in the absence of ionic wind, the displacement of the flame away from regions of high electric field (here called "repulsion") is only dependent on the electric field intensity and not on the proximity of the metallic surface. On the contrary, the displacement of the flame towards regions of high electric field (here called "attraction") is instead strongly dependent on the proximity of the electrode to the flame.

The influence of frequency on deflection is summarized in Figure 5

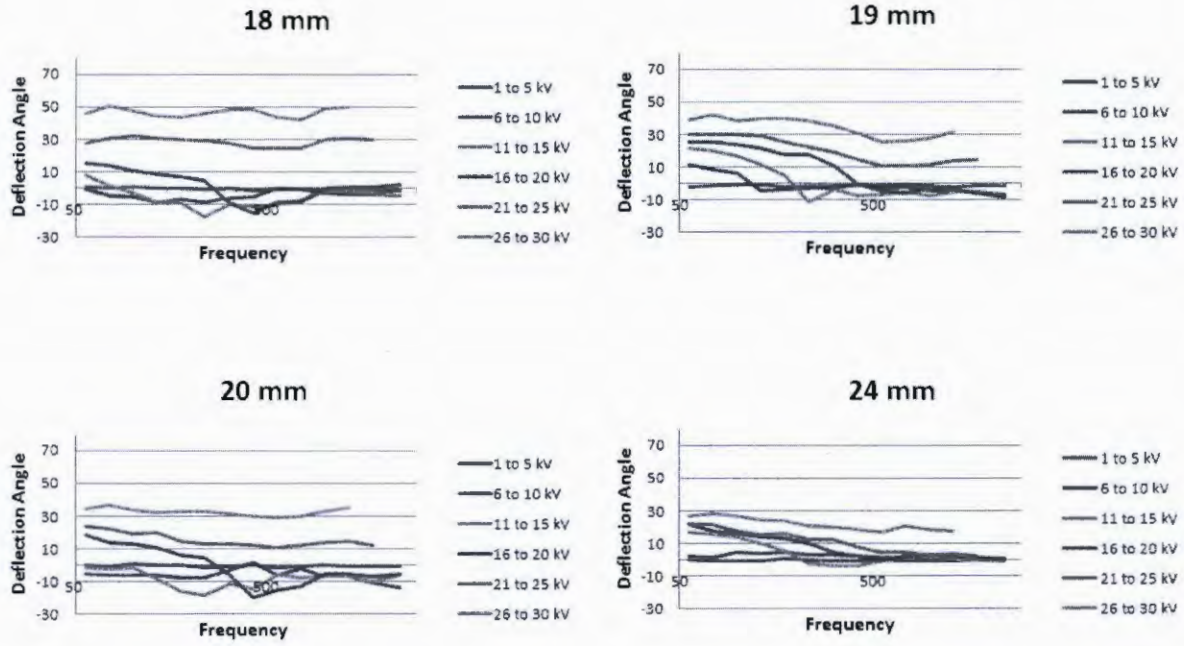

Figure 5.

Figure 5 shows plots of the deflection angle as a function of frequency of the applied field. Each plot collects data taken for a specific electrode-flame distance. The curves in each plot correspond to the average deflections in a range of voltages (defined in the legend). Irrespective of the electrode-flame distance, a general trend is observed. 1) At low voltages the "repulsion" vs frequency dependence is negative (more repulsion at low frequency). 2) At high voltages the "repulsion" vs frequency dependence is positive (more repulsion at high frequency). 3) The "attraction" appears to be associated with a dip in what could be an otherwise monotonic trend of the "repulsion". The position of this dip increases in frequency with increasing voltage.

Figure 6 shows the influence of soot on the deflection and luminosity of the flame as evidenced by our 3D plots. These results suggest that soot might play an important role in the generation of flows within the flame upon the application of an electric field.

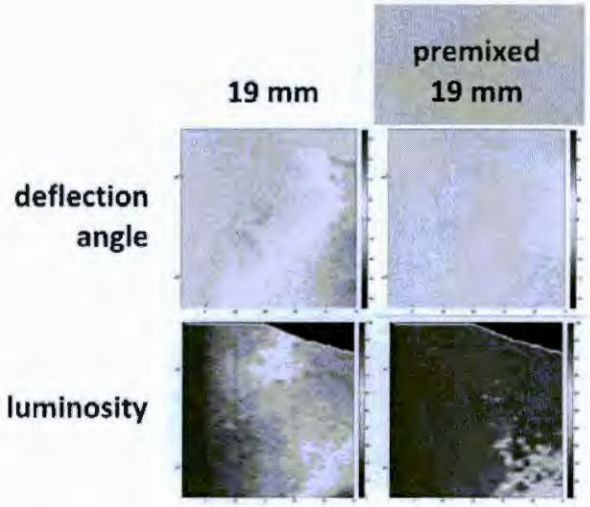

Figure 6. The effect of voltage and frequency on the deflection angle (top) and luminosity (bottom) of a non-premixed flame (left) and a premixed flame (right).

Implications for Scale Up. From these results we gathered the following information that is meaningful for scaling up these effects to larger flames, larger electrodes, larger areas. 1) The strongest effect (i.e. largest deflection) on the flame is associated with a displacement of the flame from areas of highest electric field towards regions of lower electric field. This effect occurs, in the case of a methane/air non premixed conical flame, when the field intensity at the flame is >0.5 MV/m; it increases with field intensity and with frequency. 2) At lower fields (between 0.2 MV/m and 0.5 MV/m), the flame can be driven in the opposite direction (i.e., towards regions of highest field intensity). This effect is strongly dependent, in the case of bare electrode and in the absence of corona wind, on the distance between the electrode and the flame. 3) Soot might play a fundamental role in the generation of flows within flames upon the application of electric fields upon them.

Mechanisms of Interaction of Flames with E-Fields

Summary. The previous study highlighted the importance that boundaries (e.g., the electrodes) might have on the observed effects of electric fields on flames. In this section we propose some hypothesis driven experiments on the effects that we might expect from boundaries in proximity of the flame.

Asymmetric transfer of momentum. In Figure 7 we show one hypothesis on the effect of the position of boundaries on the generation of charge-driven flows within the flame. The Figure outlines two conditions (top: V=0; bottom: $V=V_0$) of the same 1D system. The system is chosen to mimic the insulated wire design with which we observed the suppression events, where the electrode raised to high potential is close to the flame and separated from it by an insulator. The grounded counterelectrode is much further away from the flame. If we assume that i) the flame will produce a fixed amount of charges (positive and negative in equal amounts) per unit time, ii) the charges being produced have similar efficiencies in their ability to transfer momentum to neutral species by collision, and that ii) the electric field applied to the flame is large enough to extract those charges from the flame, we can easily

see that the momentum that the charged species transfer to the gas phase is very different on the two sides of the flame. The charges (positive charges, in the case depicted in Figure 7) being projected towards the furthest electrode will transfer momentum to the neutral species in the air during their entire path to the counterelectrode. The corresponding charges of opposite sign will instead travel towards the closest electrode and will impact the insulating sheath on the electrode much before the positive charges have ended their motion towards the counterelectrode. The negative charges cannot transfer any momentum as long as they are sitting on the insulating sheath. Therefore, we can expect an asymmetry in the transfer of momentum from the charged species to the neutral gas species, which could cause a steady flow of air towards the counterelectrode. This effect should occur for DC field conditions, irrespectively of the sign of the potential applied to the electrode. Experimentally, a DC potential applied to an insulated wire electrode positioned close to the flame causes a small but noticeable deflection away from the electrode that is independent on the sign of the voltage.

Charge accumulation and deflection. In the case of AC fields, a further effect might occur. The charges accumulated on the sheath would be periodically ejected upon the inversion of the potential applied to the electrode. Those accumulated charges would be ejected along the path of maximum field gradient which, in the case of a wire electrode geometry pointing at the counterelectrode, corresponds to a straight line towards the counterelectrode. We can therefore expect that the ejection of these ions at each cycle could generate a concentrated flow from the tip of the wire. Since the tip of the wire is positioned at the base of the conical flame, this flow could easily contribute to deflect and destabilize the flame.

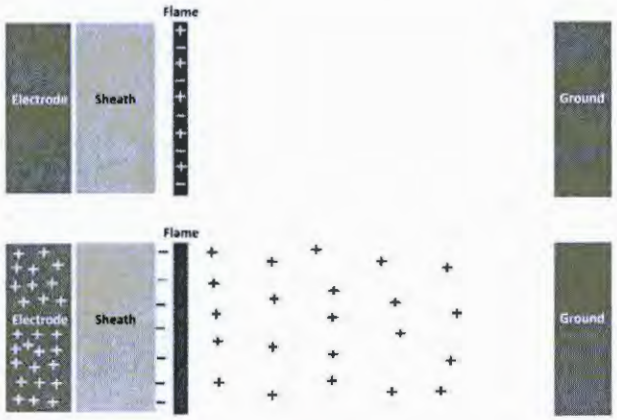

Figure 7. Sketch showing the effect of electrode geometry and proximity to the flame on the transfer of momentum from charged species to neutral gas species.

Experiment design. Experiments were designed to verify these hypotheses. Four experiments were conducted with the same electrode geometry (i.e., insulated wire electrode, plate counterelectrode). In the first two experiments (1 and 2) we applied a 40kV DC voltage to the flame. In the last two experiments (3 and 4) we applied instead an AC voltage (40kV, 1kHz). In the case of experiments 1 and 3, the application of the 40kV DC voltage to the flame (i.e., the "event" being observed) was preceded by the application of a positive 40kV DC voltage to the electrode for 30 seconds. In the case of

experiments 2 and 4, the application of the 40kV, 1kHZ AC voltage to the flame (i.e., again, the "event" being observed) was preceded by the application of a negative 40kV DC voltage to the electrode for 30 seconds. The hypothesis is that the application of a DC field can be used to accumulate charges on the insulating sheath. In Experiment 1 and 3, we expect to see a mild deflection because the same charges are being accumulated before and after the event. In Experiment 2 and 4, we expect to see a larger deflection since the charges that have accumulated before the event are ejected during the event.

Results. The results of these experiments are shown in Figure 8. Experiments 1 and 3 showed a much smaller effect than Experiments 2 and 4, as predicted. These experiments do not prove the hypothesis. For example, we have not considered the fact that different "histories" of the electrode might change the temperature at the surface of the electrode and that a different temperature might induce the formation of discharges at the surface of the electrode. Discharges would then generate a wind, much like the corona wind.

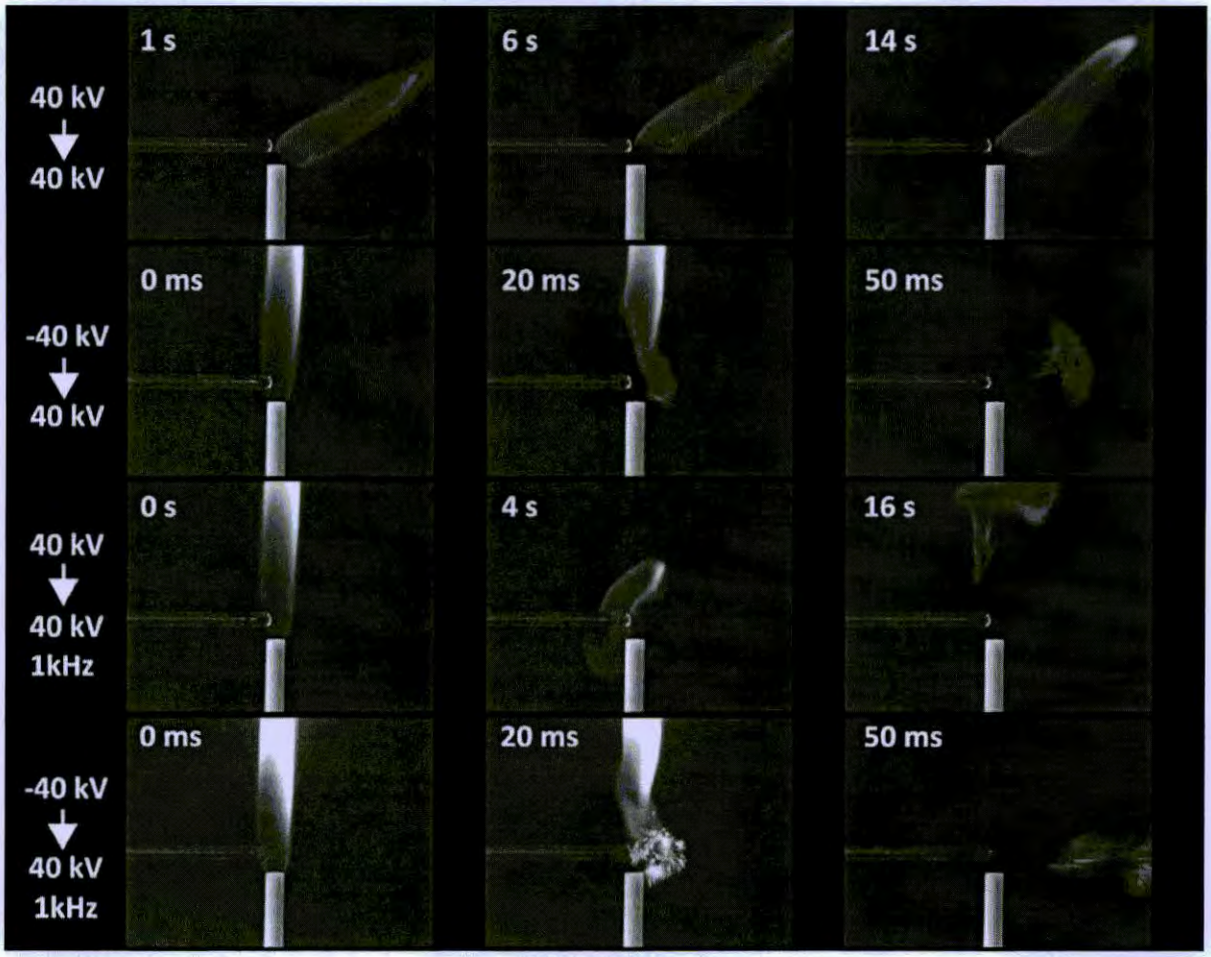

Figure 8. The effect of charge accumulation on the response of a flame to DC+ and AC fields.

Discussion. The effects of boundaries on the interaction of flames with electric fields are potentially useful. As boundaries are brought closer to the flame, new mechanisms are coming into play in the generation of flow from moving charges.

Scale Up Approaches

Summary. One of the key objectives of Phase II of the IFS program was to evaluate from a theoretical and experimental point of view the feasibility of scaling up the effects of electric fields to large flames. Previously shown results have evidenced how the suppression of flames is associated with the repulsion of the flame from areas of large field intensity (>0.5 MV/m). Since the extinction of the flame is, at least in the conditions we tested, presumably occurring by blow off, the suppression of larger flames would have to be achieved either i) by using larger electrodes or electrode arrays, or ii) by using smaller electrodes moving across the flame.

Flame Arrays. The suppression of conical non-premixed methane flames did not appear to be extremely sensitive to the flow rate (i.e. the height of the flame), as long as the size of the mouth of the burner would remain constant. In all cases, the suppression of conical non-premixed methane flames seemed to be most efficient when the electrode was either in the form of an insulated wire pointed at the base of the flame (suppression by blow off), or in the form of a thin insulated metal ribbon wrapped around the mouth of the burner (suppression by liftoff). Considering the directionality of the flows generated in these experiments, it is important to consider, beside the area of the flame, also between the depth of a flame and its width with respect to the direction of the wire electrode. Therefore, we designed a modular burner system that would allow us to change the area of the mouth of the burner as well as its geometry. This burner consisted of a modular array of glass burners connected to the same methane supply. The mouths of the individual burners were close enough (4 mm) to generate a single flame and not individual flamelets.

This modular burner allowed us to test several electrode geometries and their efficacy on suppressing flames of increasing area and differing geometry (Figure 9). Of all the geometries shown in Figure 9, the only one that showed reliable suppression is the one where the flame is only one row wide but a several rows deep, with respect to the direction of the wire electrode (shown at the very bottom of Figure 9).

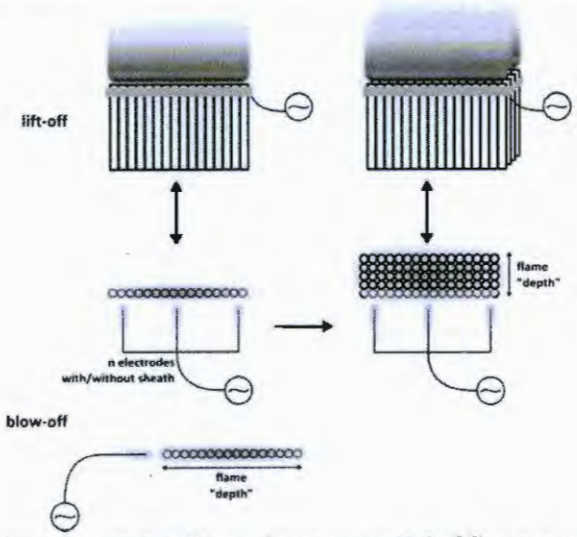

Figure 9. Experiments designed to assess the scale up potential of flame suppression by AC inhomogeneous electric fields.

Figure 10 shows the probability and time of extinction for this geometry, as a function of the depth of the flame, measured in cm. The conditions for this experiment are: fuel = CH4, non-premixed flame, oxidizer = air, voltage = 40kV, frequency = 1.2 kHz, waveform = square, insulated electrode, electrode material = Pt, electrode HoB = 6 mm, burner mouth = 3 mm, separation between burner mouths = 4mm, electrode/flame distance = 0 mm, duration of events = 30s, number of replicates = 10, flow rate of CH_4 = 370 sccm.

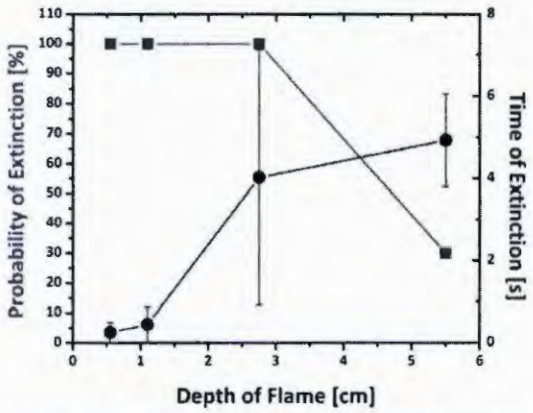

Figure 10. Flame extinction probability and times of extinction as a function of the depth of a methane/air non-premixed flame generated by an array of burners.

The results, while affected by large errors indicated unequivocally that, at the conditions of highest field and frequency allowed by our equipment, the efficiency of suppression would quickly decrease as the flame would increase in depth by a few centimeters. The large errors associated with this experiment seemed to stem from the very high sensitivity of these experiments to the orientation of the wire electrode with respect to the row of burners. Our observation was that a slight angle between the wire electrode and the row of burners would drastically decrease the suppression efficiency

Hand-Held Electrode. Since the fixed electrode approach to scale up did not yield satisfying results, even when multiple electrodes were used, we opted to test the hypothesis that scale up could be achieved by moving a single electrode across the flame. The motion of the electrode would be provided by hand. This required the design of a hand-held electrode geometry whereby the wire electrode was attached to a pole and swiped across the flame.

The results are shown in Figure 11.

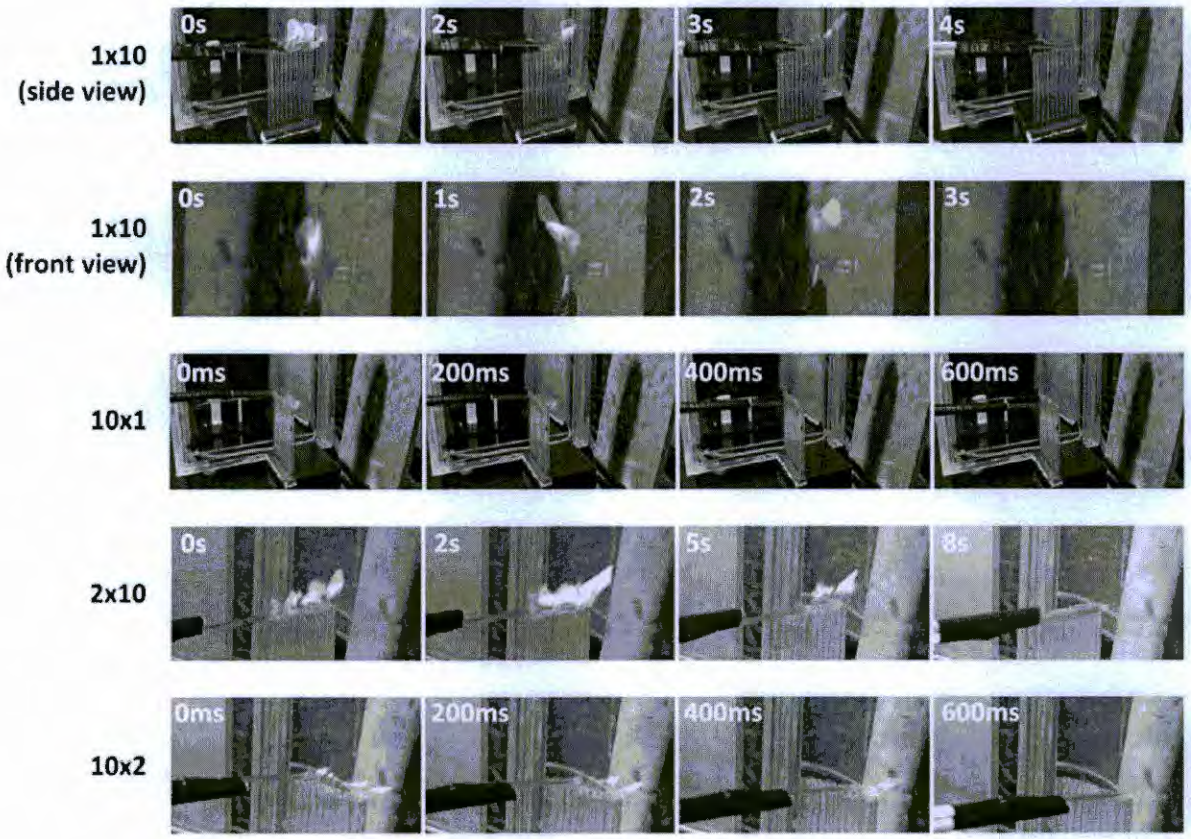

Figure 11. Snapshot of methane/air non-premixed flames generated by burner arrays and suppressed by a hand-held electrode raised to an AC potential of 40kV and 1.2 kHz.

The hand-held approach allowed to suppress 5 cm^2 flames in under a second. Two observations were interesting. i) The suppression of wide flames was much faster than that of deep flames. ii) Bare wire electrodes displaying ionic wind were not able to suppress the flames with this approach.
Soot Effects. On the basis of the previously shown results, we investigated the effect that soot might have in enhancing the effects of electric fields on flames. Figure 12 shows the effect of soot concentration on the deflection of an ethylene/methylene/nitrogen flame burning in air. The combination of gases was chosen to allow the modification of the amount of soot, while maintaining the same flow rate.

100 $^{ml}/_{min}$ CH_4	50 $^{ml}/_{min}$ CH_4	0 $^{ml}/_{min}$ CH_4
0 $^{ml}/_{min}$ H_2CCH_2	25 $^{ml}/_{min}$ H_2CCH_2	50 $^{ml}/_{min}$ H_2CCH_2
0 $^{ml}/_{min}$ N_2	25 $^{ml}/_{min}$ N_2	50 $^{ml}/_{min}$ N_2
Angle = 0	Angle = 14	Angle = 25

Figure 12. Effect of soot concentration on flame deflection.

Upon the application of an electric field to a flame, one of the charge-based processes that soot takes part in is that of bombardment charging. Since soot is electrically conductive, it will deflect the field lines of the electric field. The free charges present in the flame will then be concentrated on the surface of the soot particle. This process has been shown to increase by several orders of magnitude the mobility of soot particles in the presence of an electric field. This process largely requires the soot to be conductive. In order to control for this process we performed preliminary experiments on the doping of a methane flame with particulate. This was achieved by the setup in Figure 13.

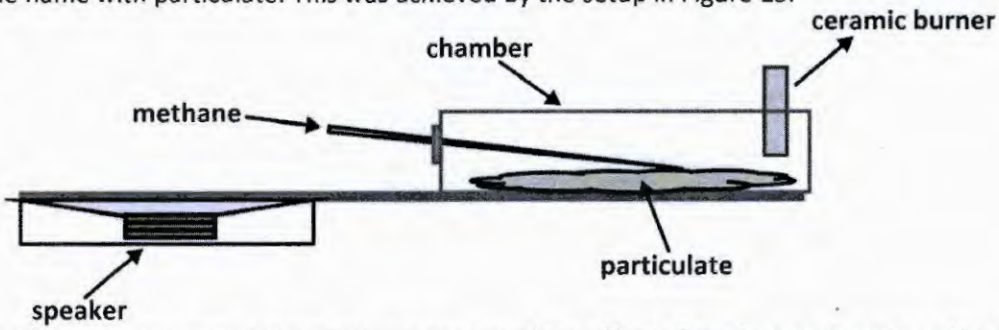

Figure 13. The apparatus used for preliminary studies of the effect of particulate dopant on the effect of electric fields on flames.

This apparatus was used to introduce two different kinds of particulate matter into the stream of burning methane: ZnO, a mostly insulating material, and carbon black, a conductive form or carbon very similar to soot. The two flames were then subjected to the same electric field and their visible deflection was considered as an indication of the magnitude of the interaction between the flame and the electric field (Figure 14).

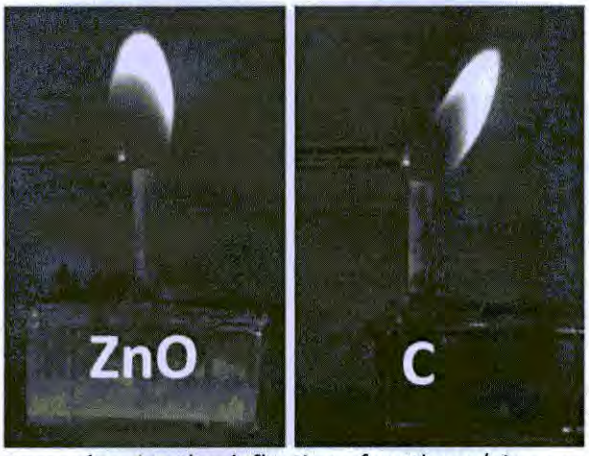

Figure 14. Two different pictures showing the deflection of methane/air non-premixed flames doped with ZnO and C powder, respectively.

The increased deflection observed for the carbon-doped flame suggests that the conductivity of the particulate could indeed be an important factor in the influence of particulate on the effects of electric fields on flames. Bombardment charging might be one of the effects that mediate the role of particles conductivity in these effects.

Pool Flames. Our previous attempt at defusing pool fires resulted in the opposite effect: the flames were amplified substantially (Figure 15 a-b). A careful analysis of the effect of electric fields on the unlit pool of fuel by photography (Figure 15 c-d) and Schlieren photography (Figure 15 e-f) showed that the fuel-air interface of the pool is made to oscillate by the electric field and that these oscillations lead to nebulization of the fuel in the gas phase. We consider this nebulization of fuel as the main cause of the amplification of pool flames in the presence of AC inhomogeneous electric fields. While this might constitute a limitation to the use of electric fields in the suppression of pool fires, it might represent an opportunity in the acceleration of combustion of liquid fuels.

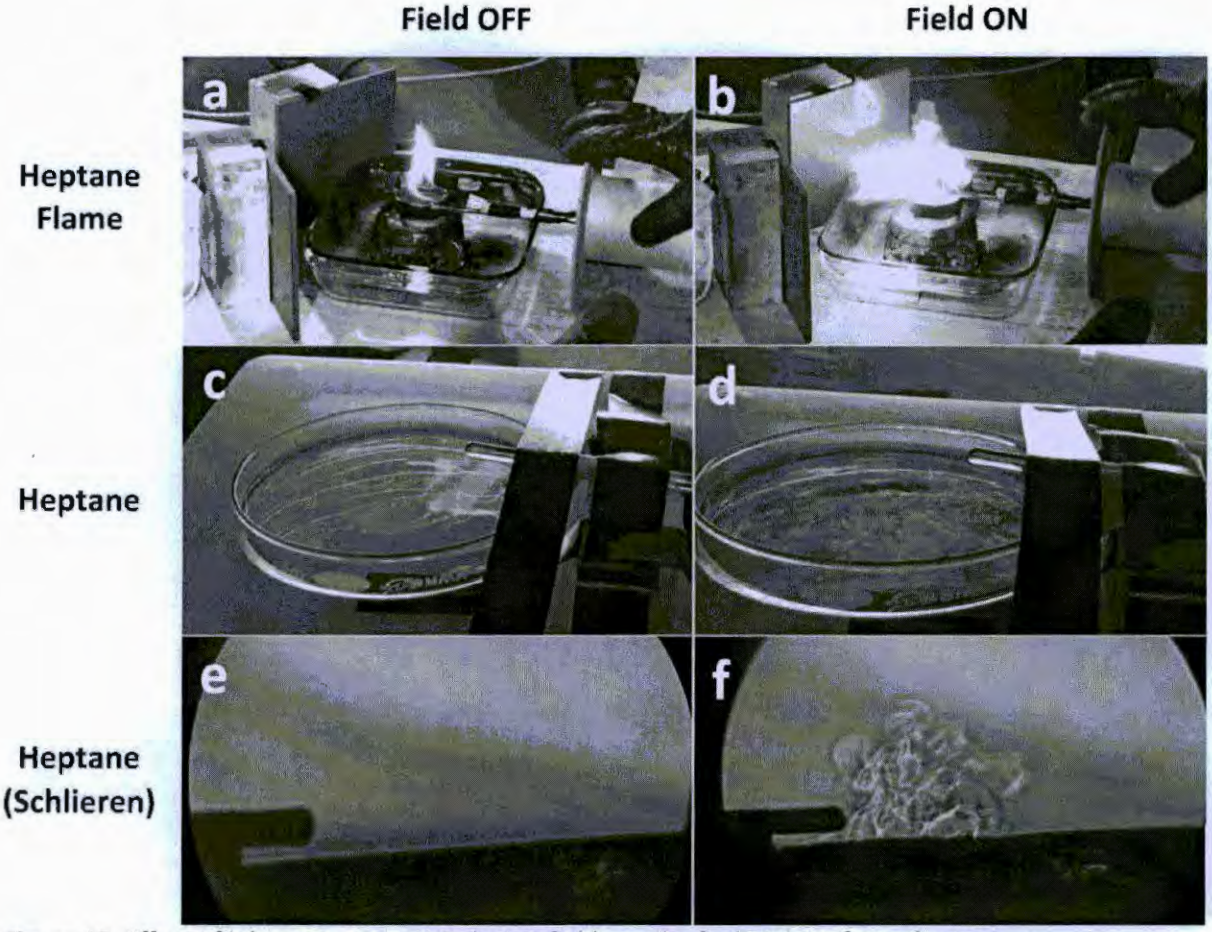

Figure 15. Effect of inhomogeneous AC electric fields on the fuel-air interface of a pool.

Distributed Electrodes. In an effort to explore possible avenues of application of electric field effects on pool flames we devised a suppression system that combines the effects of a flame arrestor and those of electric fields. This system (shown in Figure 16) is designed in an effort to design an approach that is easily deployable, scalable, and capable of suppressing pool fires. It consists of a glass container, round in shape, and open on the top. A metal mesh is glued to the opening of the container. This container simulates a double floor with an insulating bottom and a metallic mesh, separated by a gap of few centimeters. The bottom half of the container would be partially filled with a pool of heptane.
A burning pool of heptane is then poured over the mesh. In the case of the application of the field, the field is applied 4 s after the pool is poured onto the mesh. We compared the times required to extinguish flames is the presence and absence of DC or AC fields applied to the metal mesh (plot in Figure 16).
As the images and the graph in Figure 16 show, the electric field has two effects. 1) It appears to shorten the times required for extinguishing the flame. 2) It shrinks the flame down on the mesh. We furthermore observed that, right before being extinguished, the flame would propagate below the arrestor.

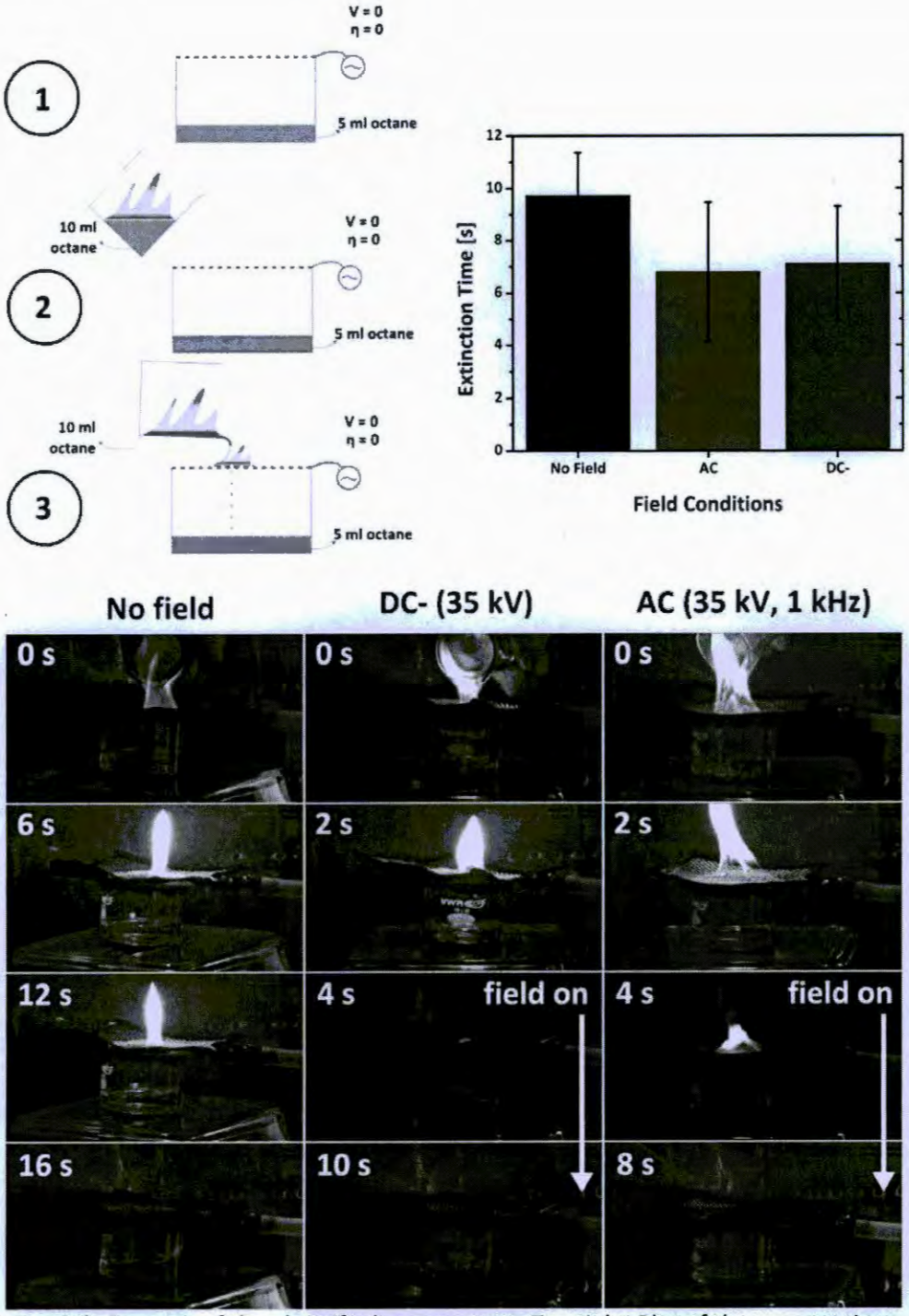

Figure 16. *Top left*. Diagram of the electrified arrestor test. *Top right*. Plot of the average times of extinction in the case of non-electrified arrestor and electrified (DC- and AC) arrestors. *Bottom*. Picture sequence of representative flame extinction events in the three conditions tested.

Scale Up Studies at Chesapeake Bay Detachment

Summary. The testing of hypotheses concerning larger pool flames could only be conducted within a designated facility outside of Harvard University, or Cambridge, MA, due to local regulations on pool flames. Our collaborators at NRL worked with us to organize a test at the Chesapeake Bay Detachment outside Washington, DC. This facility is designed to conduct large scale fire suppression tests.
In particular, we were interested in testing the effect of increasing the electric field gradients by connecting the counterelectrode to a second amplifier producing an out of phase 20kV output.
Results. A variety of field geometries were tested: insulated and bare electrodes, multiple electrodes and single electrodes, hand-held and fixed electrodes, plate counterelectrodes, double plate counterelectrodes, wire counterelectrodes.
Due to the nebulization of fuel caused by the inhomogeneous electric field, the extinction experiments were only moderately successful: out of all the geometries attempted we achieved one successful extinction event for a pool flame (single bare electrode at 40kV/1kHz, against a double counterelectrode plate at 20kV/1kHz).
Nonetheless, an important observation was obtained. As the flame was deflected by the electric field, the soot gradually deposited on the surrounding surfaces. The soot eventually started acting as a floating counterelectrode and sparks were observed between the electrode (when bare) and the soot. This observation suggests that the electric field suppression approach operates best when the flame is suppressed quickly (i.e. few seconds), thereby preventing the deposition of soot which would change the field distribution in the proximity of the flame.

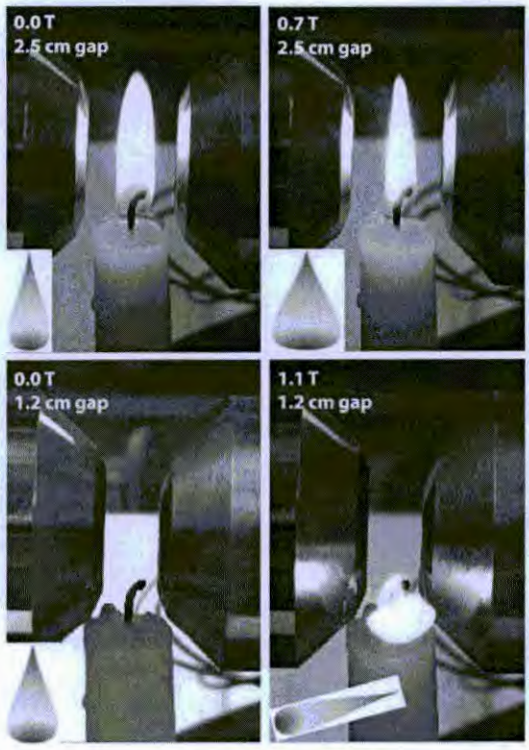

Figure 17. (*Top*) Candle flame between the poles (separated by 2.5cm) of an electromagnet at (*left*) 0T and (*right*) 0.7T field strength. (*Bottom*) The same candle between the poles (separated by 1.2cm) at (*left*) 0T and (*right*) 1.1T.

Magnetic Field Effects on Flames

Summary

We built an electromagnet yoked in iron to generate large magnetic fields. Theoretically, we can achieve a 1.5T N-S field strength; practically, however, the minimum gap size limits our field strength to ~1.1T. At these large fields, we were able to deflect diffusion flames.

Results

When we applied a field of 0.7 T (N-S), the flame sheet (from a candle flame) narrowed parallel to the magnetic field and expanded perpendicular to the magnetic field (top row of figure, below). When we applied a field of 1.1 T (N-S), the flame was deflected fully out of the pole gap (bottom row of figure, below). When we put the pole gaps close, to achieve the 1.1 T field strength, the metal poles cooled the edges of the candle flame (bottom left figure). Schematic illustrations of the side view of the flame in each figure are shown as inserts. We saw not correspondence between the direction of the applied magnetic field and the direction of the flame deflection – indicating this effect is not due to the Lorentz force on the flame.

Prior literature (Von Engel & Cozens, 1964) has shown that the magnetic susceptibility of paramagnetic oxygen could be the origin of this effect. We calculated the magnitude of the magnetic field around the electromagnet and estimated (to 1st order) the induced oxygen flow caused by this field gradient.

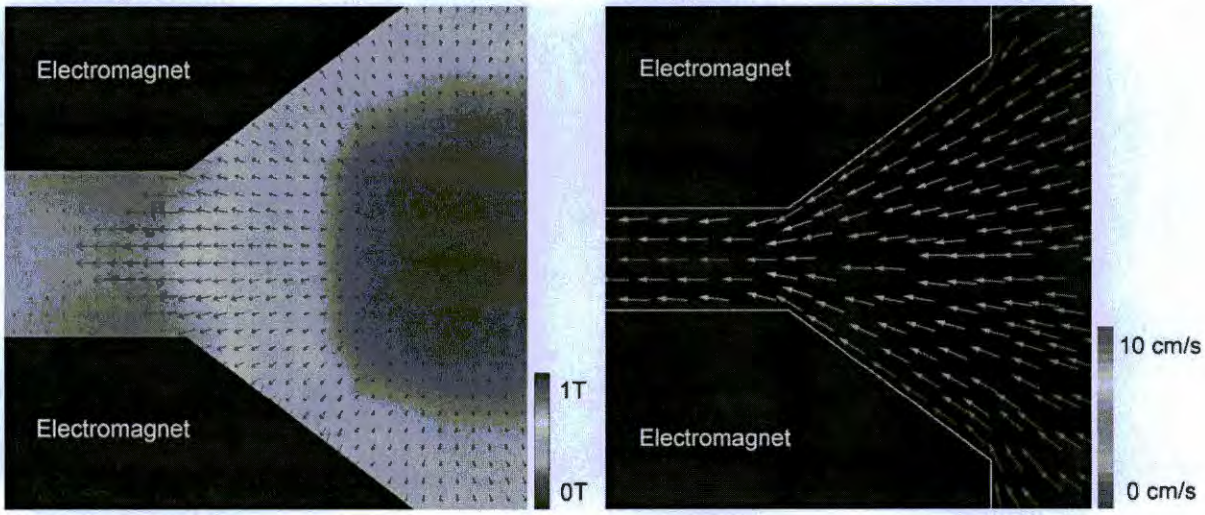

Figure 18. (*left*) Simulation of the magnitude and direction of the magnetic field around the electromagnet and (*right*) the flow rate of the oxygen, induced by the magnetic field.

These simulations suggest the flame chemistry will not affect the magnitude of the deflection from the magnetic field. To test this hypothesis, we constructed a test apparatus to deliver multiple fuel sources (methane, ethylene, and methylamine). Ethylene produces much more soot than methane when burning; yet, in a magnetic field gradient, both methane and ethylene diffusion flames have near identical deflections (Figure below; viewed looking down onto the flame).

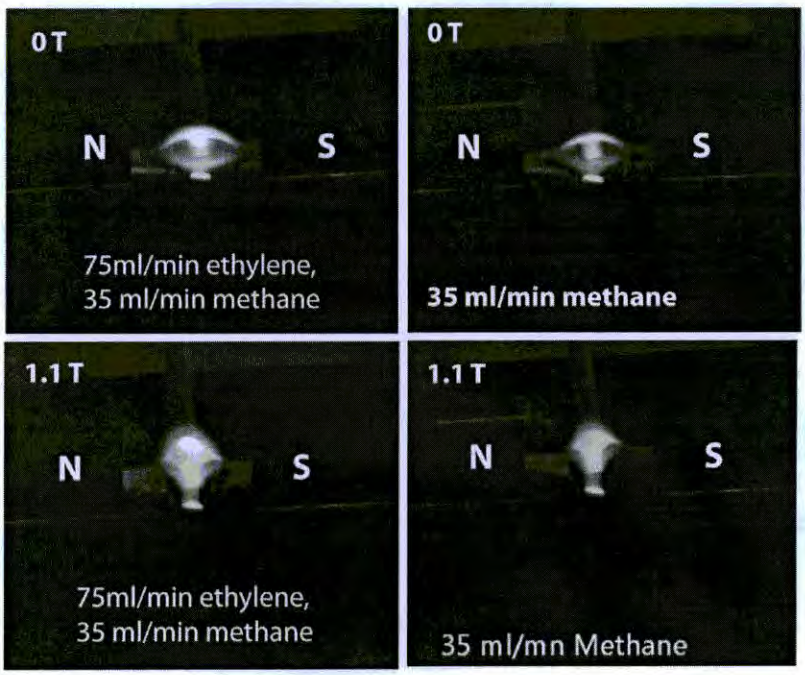

Figure 19. Diffusion flame of a (*top left)* methane/ethylene mixture and (*top right)* pure methane flow. (*bottom left)* The methane/ethylene flame under a field of 1.1T and (*bottom right*) the methane mixture under 1.1T applied magnetic field

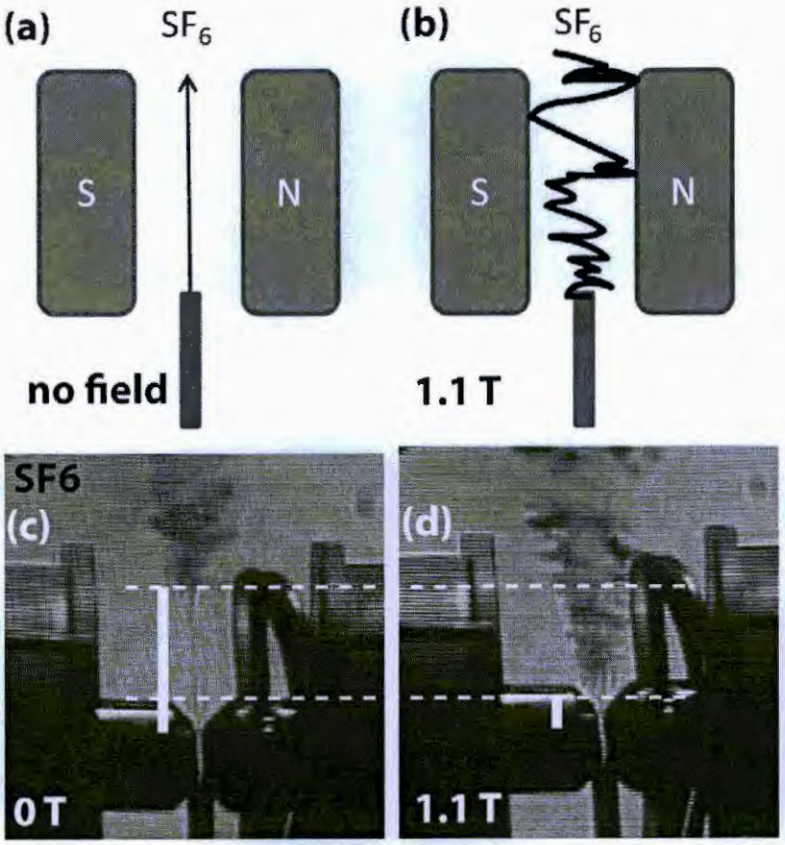

Figure 20. (a,c) Sulfur hexafluoride (SF_6) flowing between the poles of an electromagnet at 0T field strength and (b,d) SF_6 flowing between the poles of an electromagnet at 1.1T.

Finally, if the effect of the flame deflection is from induced oxygen flow, then a flame is not necessary for this effect. To demonstrate this concept, we replaced the flame with a dense gas, sulfur hexafluoride (SF_6). We imaged the flow of this gas using Schlieren imaging and showed that, with no field, there is a lengthy laminar flow region of the gas from a nozzle; however, when the magnetic field is turned on (1.1T), the laminar flow region nearly disappears. The transition from laminar to turbulent flow, triggered by the magnetic field, is in agreement with our prediction of a significant influx of another gas between the magnetic poles – the tangential flow velocities would serve to destabilize the flow of SF_6 (the dashed lines indicate the difference in height of the laminar flow region when the field is off and when it is on).

Limitations

Very high magnetic field strengths are required for significant flame deflections. Additionally, the theory we have developed indicates we are not coupling to the flame, but the oxygen in the air surrounding the flame. The current (~5 amps) required to generate the fields for the indirect manipulation of the flame appears to be inefficient compared to existing fire suppression techniques or the electrostatic/acoustic manipulations we have developed in this program.

Magnetic fields are much less susceptible to the screening effects of electrostatic systems. The ability to manipulate flames through metals, plastics, and ceramics is attractive – for suppression and enhancement of flames in engines, cockpits, and power plants. Though the magnetic susceptibility of the flames we probed in this study was negligible, these flames could be doped with particles that do couple strongly to the electromagnets.

In many situations a fire involves burning metals and other materials that are highly polarizable. Additionally, it could be possible to synthesize magnetic particles within a fire; feeding in iron(III) ethoxide could produce iron and iron oxide nanoparticles that would interact strongly with large magnetic fields. The action of synthesizing and then heating the particles would absorb heat from the flame and the magnetic field could rapidly remove the particles (and thus heat) from the fire.

Opportunities

Discussion. In conclusion, we would like to comment on potential opportunities that have arisen as a result of this effort. Oscillating electric fields are capable of generating flows within flames without requiring moving parts. These flows can overcome buoyancy and convection in shaping the flame. To an extent, electric fields can generate these flows remotely, even when the flame is separated from the source of the electric field by an insulating barrier. These flows can be more or less turbulent. Static magnetic fields are capable of generating volumes of space that are in effect "prohibited" to flames. In our observations, the effects appear to be mostly connected with the magnitude of the field gradient and with the proximity of boundaries that can accumulate and eject charged species. These two observations suggest that the optimal umbrella of application of these unique capabilities might lie with relatively small flames in well-defined confined environments.
By looking at these observations and concentrating on the general features of these new capabilities, we have obtained a handful of preliminary results that suggest a wide array of possible applications.
Prevention of propagation. The original observation that a methane/air non-premixed flame could – by the application of an oscillating inhomogeneous electric field – be prevented from propagating into a stream of unlit methane was described in the Phase I report. A hypothesis was presented (Figure 21) whereby the electric field would elicit a flow of gas propagating outwardly from the flame. This flow of gas would intercept the incoming stream of methane and deflect it away from the reaction zone.

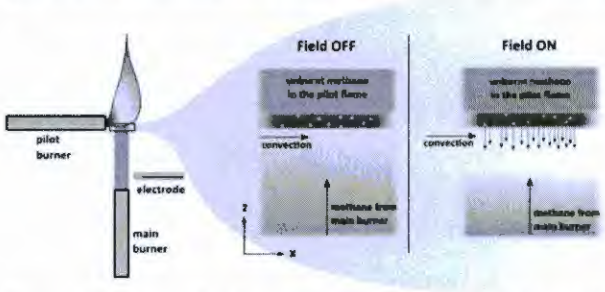

Figure 21. Hypothesis previously formulated to explain the observation of electric-field-induced inhibition of propagation.

This hypothesis was supported by an array of studies on the effect of distance of the inhibition of propagating the flame. During Phase II we verified this hypothesis by observing the event under Schlieren imaging.

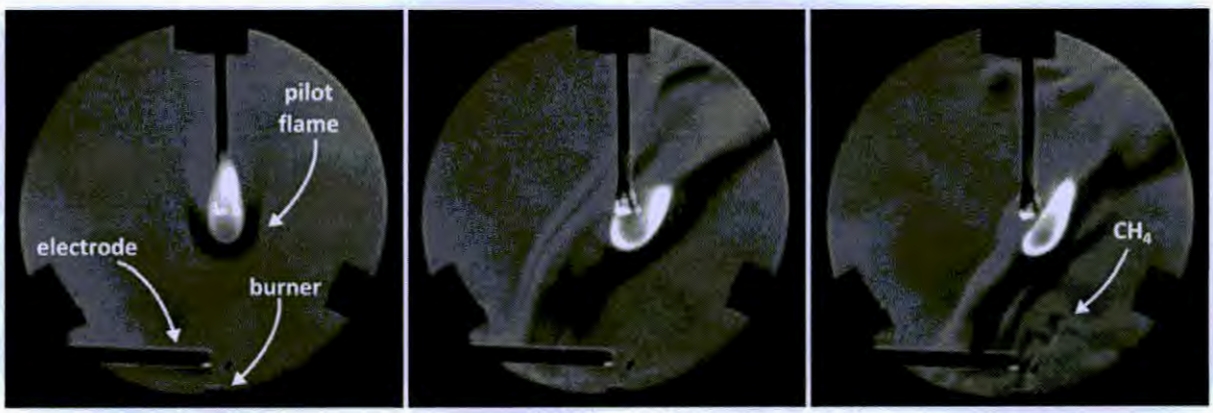

Figure 22. Schlieren imaging of a representative event of electric-field-induced inhibition of propagation

Figure 22 shows the Schlieren imaging of an event where a pilot flame is positioned above a burner. The insulated wire electrode is pointing at the base of the burner. Initially no methane is evolved from the burner. The field is turned on (middle panel of Figure YY). The ripples shown in the Schlieren image highlight the formation of flows of air at different temperatures generated around the flame through the action of the charges. The methane is then evolved from the burner, while maintaining the electric field on. As shown in the right panel of Figure YY, the methane is visibly deflected from its upward trajectory of collision with the pilot flame by the flows generated by the electric field. This deflection is sufficient to delay the propagation of the flame into the methane stream by as much as several tens of seconds.

Enhanced rate of burning. As previously shown, the application of an inhomogeneous oscillating electric field in proximity of a pool flame causes an amplification of the burning, currently attributed to the electrophoretically-driven nebulization of the liquid fuel. This enhancement in the rate of burning was particularly evident when using small pool flames. One of the characteristics of this approach is that is does not require moving parts (e.g., a piezo, a fan).

Enhanced combustion efficiency. As previously shown, the application of strong and low frequency oscillating inhomogeneous electric fields suppressed substantially the luminosity of the flame in the visible range of the electromagnetic radiation. Most of that radiation originating from the flame is attributed to black body radiation from soot particles. As outlined before, the decrease of luminosity of the flame could be attributed, for example, to i) an ejection of charged soot particles from the reaction zone of the flame that prevents the soot from becoming sufficiently hot, or to ii) a decrease in the production of soot resulting from the enhanced mixing provided by the charge-driven flows generated by the electric field. The last hypothesis is consistent with the increase in the turbulence of the flows within and around the flame when the frequency of the applied field is decreased below ~100 Hz. If this hypothesis results in being correct, it would imply that the electric field has bettered the efficiency of combustion of a non-premixed flame. There are a multitude of important technologies (e.g., diesel engines, coal-fired power plants) that make use of non-premixed combustion from relatively small flames in confined environments in order to generate energy. We are especially keen on suggesting, in this instance, that diesel engines and coal-fired power plants could represent the most meaningful target technologies for such an application of electric-field-driven flows in non-premixed flames.

Enhanced output of the flame. While the luminosity of the flame was found to diminish in the presence of an electric field, we found that an electric field could concentrate the heat released from a flame in

contact with a surface. This capability leads to the possibility of using flames for i) concentrating the heat released by the flame on a smaller area of a surface, and for ii) generating temperatures on solids that are higher than those you could normally achieve with the same flame without the electric field. Both of these capabilities are meaningful for a variety of applications, such as, for example, in welding.

The results from our preliminary experiments are shown in Figures below. The setup consisted of a burner flowing ~1L/min of methane. The methane generates a non-premixed methane/air flame which is arrested by an horizontally placed thick metal grid. The grid was used as the ground of the open electrical circuit, while an insulated metallic ring applied at the mouth of the burner was used as the electrode. Without E field, the highest temperature observed on the top of the grid via a IR camera was 631 C. Upon applying 18kV at 100Hz to the open circuit, the temperature increased rapidly by ~100 degrees to ~731 C within 40 seconds. In these field conditions, mild sparking occurred. We verified that sparks are not the dominant source of concentrated heat in this experiment by decreasing the voltage to 9kV at 100Hz (a voltage at which no sparking occurred). At this lower voltage, the temperature still increased by 50 degrees in ~40 seconds. Importantly, DC fields were not applicable in this fashion as they would generate, for the same field strengths, continuous arcs.

100 Hz at 18 kV

Field Off

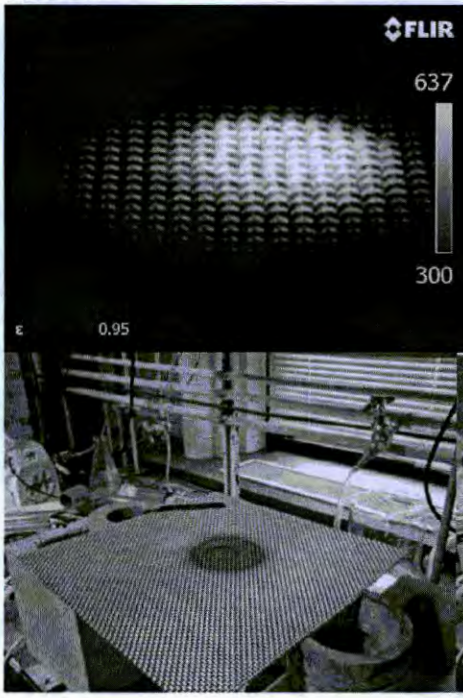

Field On

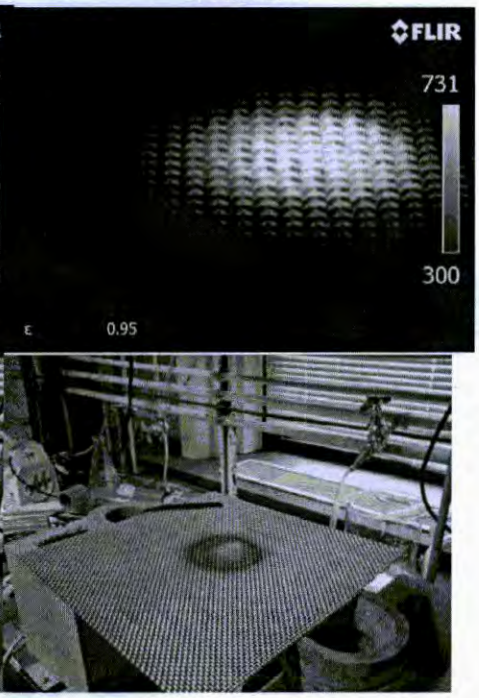

100 Hz at 9 kV

Field Off

Field On

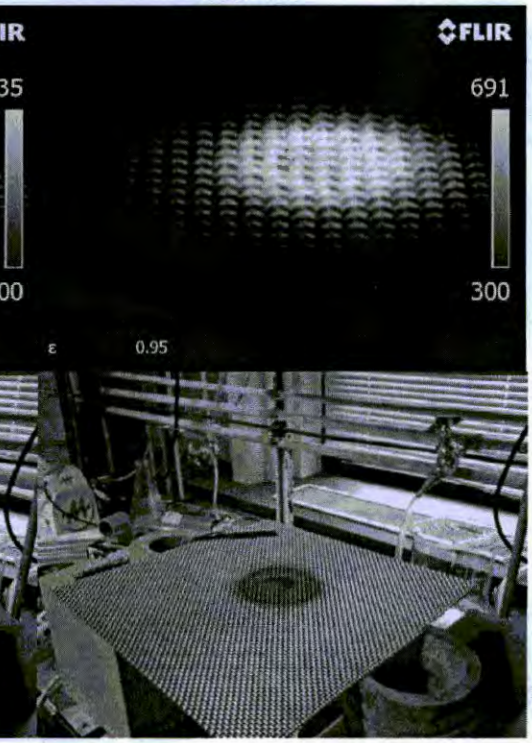

References

1 Fialkov, A. B. Investigations on ions in flames. *Progress in Energy and Combustion Science* **23**, 399-528, doi:10.1016/s0360-1285(97)00016-6 (1997).

2 Lawton, J. & Weinberg, F. J. *Electrical aspects of combustion*. (Clarendon Press, 1969).